

Structures of Silica-Mesoporous Crystals and Novel Mesoporous Carbon-Networks Synthesized within the Pores

O. Terasaki^{1,*}, Z. Liu², T. Ohsuna³, T. Kamiyama³, D. Shindo², K. Hiraga³,
S. H. Joo⁴, T.-W. Kim⁴ and R. Ryoo⁴

^{1*}*Department of Physics and CIR, Tohoku University, Sendai 980-8578, Japan.*

FAX: +81-22-217-6472. E-mail: terasaki@msp.phys.tohoku.ac.jp

²*Institute of Multidisciplinary Research for Advanced Materials, Tohoku University, Sendai 980-8577, Japan*

³*Institute for Materials Research, Tohoku University, Sendai 980-8577, Japan*

⁴*National Creative Research Initiative Center for Functional Nanomaterials and Department of Chemistry, KAIST, Daejeon, 305-701, Korea.*

Summary: After three-dimensional structures of mesoporous crystals have been solved, these crystals can be used as molds to design and synthesize nano-structured materials utilizing the available spaces within the microporous crystals. The designed nano-structured materials can be further utilized as molds, to create new meso- or nano-structured materials. Thus the nano-network structures are basically controlled by the geometries of spaces available within the mesoporous materials used, and this route opens new field for synthesis of novel nano-structured materials, which, otherwise, can not be synthesized directly on their own. To date, several ordered carbon and Pt nano-networks have been synthesized from silica-mesoporous crystals. During our studies, by close structural investigation employing electron microscopy (EM), we observed new structural features in these materials. Here, we discuss the structural features from both atomic and mesoscopic scales and possibilities to control their fine structures for further usage.

Introduction

Mesoporous crystals, using surfactant molecules synthesized either from layered silicate or water soluble silica source[1,2], have attracted considerable attentions in various fields. Recently, we have developed a method to solve three-dimensional (3d-) structure of mesoporous crystals uniquely from Fourier analysis of a set of HREM images, which is one of the electron crystallography (EC) methods[3,4]. We have solved several 3d-structures of mesoporous-silica crystals which include MCM-48, SBA-1, SBA-11, SBA-12, SBA-15 and SBA-16 [3-5]. From these structural studies it is evident that these materials possess uniform nanoporous spaces which are ideal to employ as molds for the synthesis of nano-structured materials. The greatest advantage of these mesoporous crystals is that their pore dimensions can be finely controlled by a choice of amphiphilic molecule and its concentration. In addition, subsequent to the preparation of nan-structured materials, the molds can be easily removed. Based on our structural studies, several nano-structured materials such as carbon and Pt networks have been successfully synthesized within silica mesoporous crystals of MCM-48, SBA-1 and SBA-15 [6-9].

In this report, we will begin with importance of phase in crystal structure factor, principles of diffraction and imaging (EC) before discussing the structure determination and characterization procedures by taking examples of silica-mesoporous crystal MCM-48 and carbon networks CMK-1 and CMK-4. Structural details of SBA-15 and carbon networks, CMK-3 are also discussed.

Phase of crystal structure factor, Babine's principle and CMK-4

The crystal structure factor for g -reflection, $F(hkl)$ where g is given by index of hkl in reciprocal space, is g -th component of Fourier transformation of the structure. $F(hkl)$ is generally complex and described by $F(hkl) = \text{Amp}[F(hkl)]\exp[i\alpha(hkl)]$, where $\text{Amp}[F(hkl)]$ and $\alpha(hkl)$ are amplitude and phase terms for g -reflection, respectively. If the crystal has a center of inversion, then $\alpha(hkl)$ is either 0 or π by taking the origin of coordinates at the inversion center. HREM image carries both the amplitude and the phase information, while diffraction intensity gives only the amplitude term. Once we have a complete 3d-data set of the factors from analysis of HREM images, the structure can be determined uniquely and straightforwardly by an inverse Fourier transformation.

The structure of the silica wall of MCM-48, which was filled with surfactant

rods, obtained from EC is shown in Fig. 1. After removing the surfactant by calcination, carbon networks (prepared from different carbon sources, see ref. for details of the preparation) were formed uniformly within the mesopores of MCM-48. These nano-structured carbons obtained by complete dissolution of silica MCM-48 are designated as CMK-1 and CMK-4. HREM images of silica MCM-48 and CMK-4 together with Fourier diffractograms obtained from the images are shown in Fig. 2 for $[-111]$

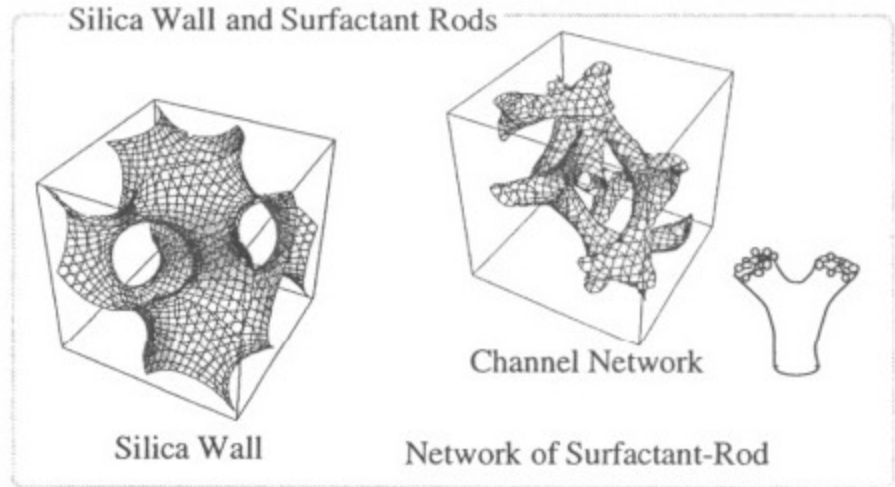


Fig.1 Structure solution obtained from EC for MCM-48, silica wall and channel structure.

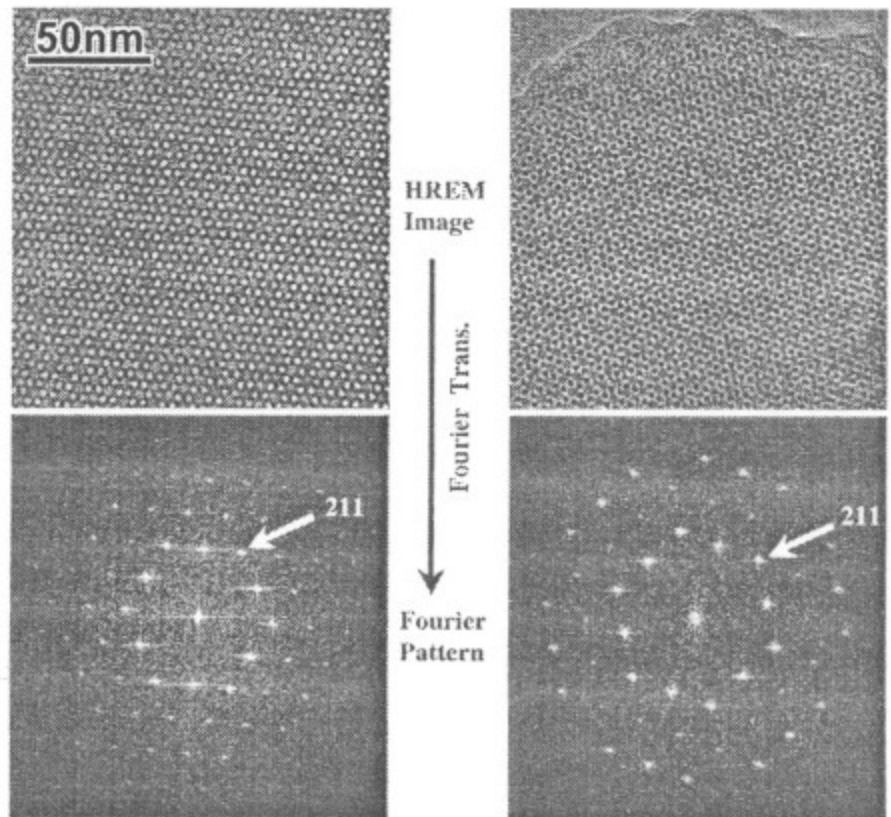


Fig.2. HREM images of $[-111]$ incidence and their Fourier diffractograms. MCM-48 (left) and CMK-4 (right).

incidence. It is apparent from the contrast in the HREM images of MCM-48 and CMK-4 (Fig. 2) they are opposite to each other. Although the structures of MCM-48 and CMK-4 are different and complement to each other, as shown in Fig. 1, both have the same symmetry, $Ia-3d$, and give same Fourier diffractograms shown in Fig. 2. The structures shown in Fig. 1 (as silica wall and network of surfactant-rod) are two solutions out of many possible structures, which give the same diffraction pattern as shown in Fig. 2. This comes from the differences in the phases of crystal structure factors, which clearly indicates the importance of phases to give structure solutions. The crystal structure factors of MCM-48 and CMK-4, obtained from EC, are shown in the Table below. If we assume that the silica wall and the carbon rods have the same scattering density, it is obvious from the table that, the amplitudes of crystal structure factors for hkl reflection are same but the phases are anti-phase, which is known as Babine's principle in optics. Therefore if the mesopores are occupied completely by the material with uniform and equal scattering density as the silica wall, then we cannot observe any density modulation except the uniform scatterer of crystal shape, which gives only shape-function information at very close to the origin, 000, in reciprocal space. This is the reason why intensity of Bragg peaks representing mesostructures will be diminished when the mesopores are filled, which is typically observed in many powder XRD patterns (see Fig. 3b).

hkl	d/nm	MCM-48		CMK-4	
		Amp.	Phase	Amp.	Phase
211	3.52	100.	π	100	0
220	3.04	43.6	π	41.7	0
321	2.30	4.1	0	5.3	π
400	2.15	14.5	0	9.7	π
420	1.92	10.7	0	4.6	π
332	1.83	13.5	π	6.5	0
422	1.75	5.3	π	2.2	0
431	1.69	3.4	π	0.6	0

Symmetry change in CMK-1

It is interesting to note that a new reflection {110} is observed for CMK-1 (see Fig. 3(e)), which was not observed for the material and are not allowed in $Ia-3d$, is observed for CMK-1. The HREM image of CMK-1 shows domain character. In addition the image taken with the [111] incidence shows deviation from three-fold symmetry, therefore it is clear that CMK-1 is not cubic. The Fourier diffractogram of the HREM image of CMK-1 taken with the [110] incidence indicates that CMK-1 keeps 4_1 symmetry along the c direction, which is a part of the symmetry element of $Ia-3d$, and thus CMK-1 is tetragonal. The unique axis of tetragonal can be either [100] or [010] or [001] of cubic and therefore CMK-1 consists of small domains. This also explains an appearance of a cubic system in unit cell size as an average structure within our experimental resolution. Tetragonal $I4_1/a$ is the most probable space group. To explain the powder XRD and ED patterns, crystal structure factors for several reflections were calculated as a function of magnitude for mutual displacement along the [100] based on

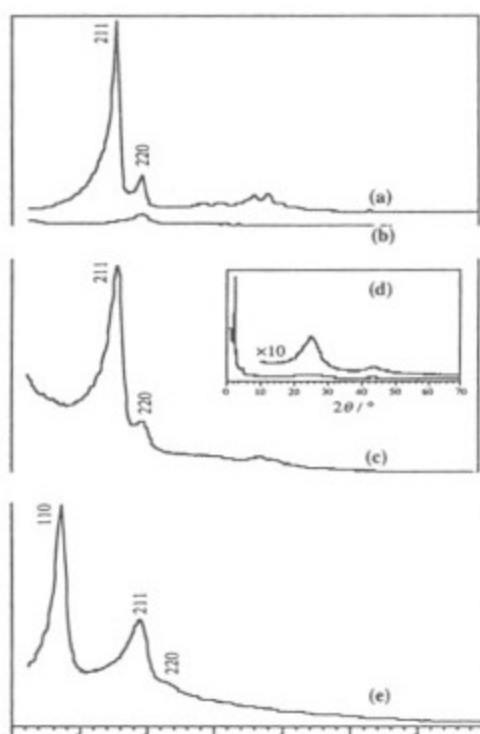


Fig. 3. Powder XRD pattern with Cu K_{α} . MCM-48 (a), MCM-48/CMK-4 (b), CMK-4 (c) and CMK-1 (e).

